

Carbon nanotube sheets as electrodes in organic light-emitting diodes

C. M. Aguirre

Regroupement Québécois sur les Matériaux de Pointe, and Département de Génie Physique, École Polytechnique de Montréal, Montréal, Québec H3C 3A7, Canada

S. Auvray

Regroupement Québécois sur les Matériaux de Pointe, and Département de Chimie, Université de Montréal, Montréal, Québec H3C 3J7, Canada

S. Pigeon

OLA Display Corp., Montréal, Québec H3C 3R7, Canada

R. Izquierdo

Département d'Informatique, Université du Québec à Montréal, Montréal, Québec H3C 3P8, Canada

P. Desjardins

Regroupement Québécois sur les Matériaux de Pointe, and Département de Génie Physique, École Polytechnique de Montréal, Montréal, Québec H3C 3A7, Canada

R. Martel^{a)}

Regroupement Québécois sur les Matériaux de Pointe, and Département de Chimie, Université de Montréal, Montréal, Québec H3C 3J7, Canada

(Received 27 January 2006; accepted 29 March 2006; published online 1 May 2006)

High performance organic light-emitting diodes (OLEDs) were implemented on transparent and conductive single-wall carbon nanotube sheets. At the maximum achieved brightness of 2800 cd m^{-2} the luminance efficiency of our carbon nanotube-based OLED is 1.4 cd A^{-1} which is comparable to the 1.9 cd A^{-1} measured for an optimized indium tin oxide anode device made under the same experimental conditions. A thin parylene buffer layer between the carbon nanotube anode and the hole transport layer is required in order to readily achieve the measured performance. © 2006 American Institute of Physics. [DOI: 10.1063/1.2199461]

Light-emitting diodes made from thin organic and polymeric layers are generating much excitement due to their applicability in large area flat panel displays and solid state lighting.¹ It is known that the performance of organic light-emitting diodes (OLEDs) is largely dominated by charge injection from the anode and cathode.² In addition to influencing the overall brightness and power efficiency, improving charge injection increases the lifetime and stability of these devices.³ The choice of the appropriate electrode material is thus paramount to obtaining reliable and efficient OLEDs.

Up to now only transparent conducting oxides, such as indium tin oxide (ITO), display both the transparency ($>80\%$ in the 400–700 nm region) and resistance ($\sim 20 \Omega/\text{sq}$) needed for the electrodes through which light is extracted.⁴ However, in spite of all the work that has been done towards optimizing devices implemented on ITO anodes, their use poses important limitations. Indium migration from the ITO surface is a known cause of premature device failure.^{3,5} Furthermore, ITO does not lend itself well to deposition onto flexible substrates.⁶ The low temperature deposition techniques that are compatible with polymeric substrates lead to higher sheet resistances and surface roughness values. Moreover, repeated bending of ITO layers inevitably leads to cracking and delamination. Finally, the fabrication of top emitting devices using ITO anodes is limited as the ITO deposition process often damages the underlying organic semiconducting layers.⁷

Thin and flexible carbon nanotubes sheets exhibiting excellent optical transparencies (40%–90%) and electrical conductivities ($\sim 1 \times 10^4 \text{ S cm}^{-1}$) have recently been fabricated using a room temperature deposition technique.⁸ Their intrinsic work function (4.5–5.1 eV)^{9,10} is similar to that of ITO (4.4–4.9 eV)¹¹ and can be tailored through both *n*-type and *p*-type charge transfer doping,¹² allowing, in principle, double-sided charge injection in transparent OLEDs. Recently, a polymer LED¹³ and an organic solar cell¹⁴ that used multiwall carbon nanotube and single-wall carbon nanotube (SWNT) anodes, respectively, were demonstrated.

In this letter, we show that SWNT sheets can be used as hole injecting anodes for high performance small molecule OLEDs. The luminance efficiencies of our devices are comparable to conventional geometry ITO-based OLEDs made under the same experimental conditions. Our results convincingly demonstrate that carbon nanotube anodes are a viable alternative to transparent conducting oxides.

The SWNTs used in these studies were produced by a pulsed laser vaporization technique¹⁵ and purified following a standard procedure.¹⁶ This involves the refluxing of the as-received soot in concentrated nitric acid (60%) for 4 h followed by filtration and subsequent refluxing in ultrapure water for 2 h in order to remove any excess acid. These purification steps eliminate amorphous carbon and metal catalyst impurities from the sample and result in the *p*-type charge transfer doping of carbon nanotubes.⁸

Carbon nanotube sheets are made following the procedure recently described by Wu *et al.*⁸ The purified SWNTs are dispersed in a 2% sodium cholate solution and centri-

^{a)}Electronic mail: r.martel@umontreal.ca

fused at 5000 g for 2 h in order to remove undispersed particles and large nanotube bundles. Carbon nanotube sheets of increasing thicknesses are made by filtering increasing volumes of a 1×10^{-4} mg ml $^{-1}$ sodium cholate solution through a 0.2 μ m cellulose filter. Finally, the sheets are transferred onto clean glass slides by dissolving the filters in acetone.

OLEDs were fabricated on carbon nanotube electrodes as well as on commercial ITO-coated glass substrates (Colorado Concept Coatings LCC, 20 Ω /sq). The carbon nanotube electrodes are patterned through a shadow mask from a 130 ± 12 nm thick carbon nanotube sheet (60 Ω /sq) by reactive ion etching using a rf oxygen-plasma (30 s, 75 mTorr, 80 mW/cm 2). Patterning the electrodes in this manner is done in order to avoid the rough edges that would result from cutting the sheets using other methods, e.g., scissors. Finally, electrical contacts are made by evaporating a 50 nm thick Ti layer to one end of the nanotube electrodes.

Traditional OLED devices were fabricated on oxygen-plasma treated ITO anodes. The organic stack structure was optimized for maximum luminance efficiency and consisted in a 10 nm copper phthalocyanine (CuPc) hole injection buffer layer (HIL), a 50 nm *N,N'*-bis-(1-naphthyl)-*N,N'*-diphenyl-1,1-biphenyl-4,4'-diamine (NPB) hole transport layer (HTL), and a 50 nm tris-(8-hydroxyquinoline) aluminum (Alq $_3$) electron transport and emissive layer deposited at ~ 0.1 – 0.2 nm s $^{-1}$ in a thermal evaporator with a base pressure of 5×10^{-6} Torr. The cathode was made by evaporating 1 nm of lithium fluoride and 50 nm of aluminum immediately following the organic layer deposition (i.e., without breaking vacuum). As will be discussed below, thicker organic layers and an alternative buffer layer material were determined to be necessary in order to achieve high performance OLEDs on SWNT electrodes. The buffer layer consisted in an ~ 1 nm parylene-C coating (Cookson CVD deposition system) applied onto the carbon nanotube sheets prior to organic stack deposition. OLED devices were then made by depositing NPB and Alq $_3$ layers of equal thicknesses followed by the same bilayer cathode. Although both 50 and 100 nm organic layer thicknesses were attempted, devices consisting of thicker layers displayed the best performance. The emissive area of all devices shown is 10 mm 2 .

The device measurements were carried out under a nitrogen atmosphere using a semiconductor parameter analyzer (HP 4145A) and a photometer (Delta-Ohm HD9021) controlled by data acquisition software.

The four-point probe sheet resistance of the SWNT electrodes is plotted in Fig. 1 as a function of their transmittance at $\lambda = 520$ nm, i.e., the peak emission wavelength of our devices. As expected, an increase in transmittance is obtained at the cost of an increase in sheet resistance. The corresponding conductivity ($\sim 1.2 \times 10^3$ S/cm) is constant across the thickness range indicating that, in spite of the high surface roughness of 12 nm (rms) measured for all sheets [determined by atomic force microscopy (AFM)], a continuous percolative carbon nanotube network is formed even for the thinnest sheets fabricated. This conductivity value, which depends sensitively on carbon nanotube source and doping treatments, falls within the range of reported values.^{8,13,14}

The quality of the small molecule/SWNT interface is a key element for the efficient fabrication of OLED devices on SWNT electrodes. The considerable roughness of the SWNT sheets imposes a lower limit to the thicknesses of the organic layers. AFM images (not shown) immediately following the

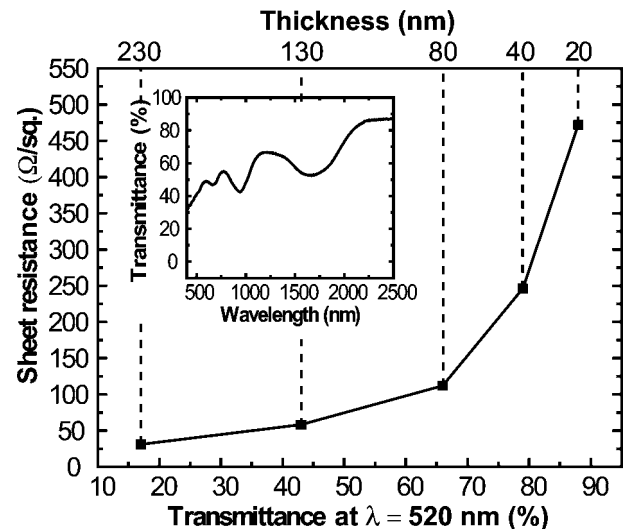


FIG. 1. Sheet resistance as a function of the optical transmittance at $\lambda = 520$ nm for carbon nanotube sheets of different thicknesses. Also shown in the inset is the visible and near-infrared transmission spectrum for the 130 nm thick sheet used in the SWNT OLED.

deposition of 100 nm thick NPB layers on bare SWNT electrodes revealed the presence of large pinholes (~ 100 nm) arising from inappropriate organic layer coverage. This in turn led to devices that were electrically shorted. A parylene buffer coating dramatically improved the wetting and adhesion of the organic layer and led to essentially complete electrode coverage.

A cross sectional image ($\sim 20^\circ$ inclination) of the complete SWNT-OLED device is shown in Fig. 2. The sample was prepared for scanning electron microscope (SEM) imaging by cleaving the glass substrate at the center of the emissive area. Given the flexible, fabric quality of the interconnected carbon nanotube network, the sheet does not break at the substrate edge. It can be seen that the SWNT sheets are torn and fold onto the glass substrate.

The current density and luminance characteristics of the devices as a function of voltage, displayed in Fig. 3, are similar for both devices and are typical of OLEDs.^{1,4} Despite the thicker organic layers used, the measured turnon voltage (6.6 V) for our SWNT-OLED is only slightly higher than

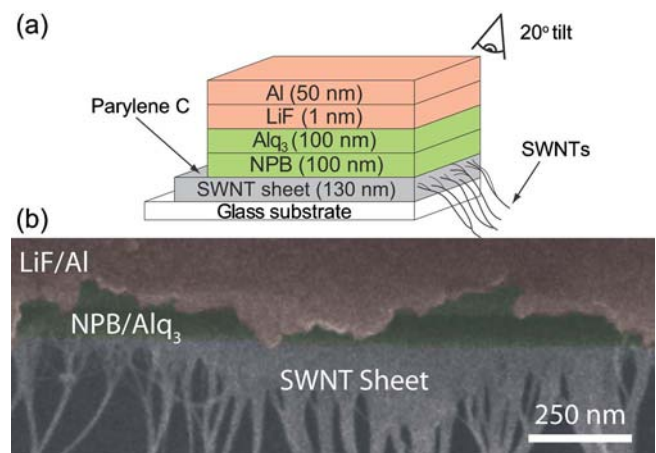


FIG. 2. (Color online) (a) Schematic of the SWNT OLED device and (b) corresponding cross sectional scanning electron microscopy image at a broken edge taken at a 20° angle from the surface normal. Color was added to the image for clarity.

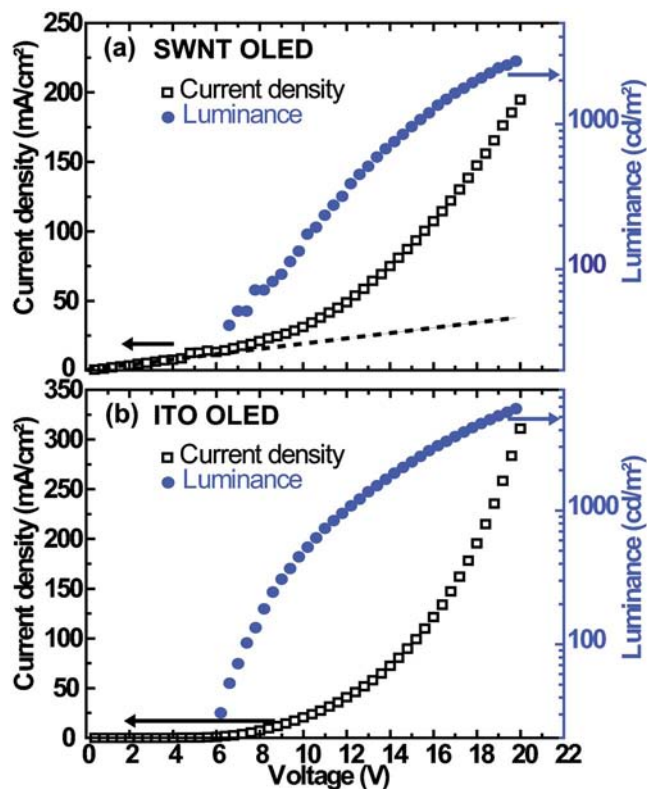


FIG. 3. (Color online) Current density (squares) and luminance (circles) as a function of applied voltage for OLEDs fabricated (a) on carbon nanotube anodes (SWNT-OLED) and (b) on oxygen-plasma treated ITO anodes (ITO-OLED).

that measured for the thinner ITO-OLED (6.2 V). The maximum achieved brightness is 6000 cd/m^2 for the ITO-OLED compared to roughly half, 2800 cd/m^2 , for the SWNT-OLED. This is remarkable given that the carbon nanotube anode displays a transmittance at the peak emission wavelength that is approximately half that of the ITO/glass substrate (i.e., 44% and 90%, respectively). After accounting for optical absorption losses, both devices exhibit similar emission performances.

As shown in Fig. 3(a) in the case of the SWNT-OLED, below the device turnon, the current increases linearly with voltage indicating the presence of leakage currents. By extrapolating this curve [dotted line in Fig. 3(a)] we estimate that, at the maximum achieved brightness, 20% of the current does not participate to the electroluminescence. Nevertheless, in spite of observed current and optical absorption losses, the luminance external efficiencies achieved are significant. At the maximum light output (20 V) they are comparable at 1.9 and 1.4 cd A^{-1} for the ITO-OLED and SWNT-OLED, respectively. We can therefore expect that, by improving the conductivity/transparency ratio and by eliminating all current losses, the performance of SWNT-OLED devices will exceed that of ITO-OLEDs.

Buffer layers between the ITO anode and the HTL are routinely used in order to increase the overall performance of ITO-based OLEDs. The exact role of this layer is, however, not well understood.¹⁷ Parylene, in our case, was chosen for its ability to form thin conformal coatings on carbon nanotubes.¹⁸ The introduction of this insulating layer between the anode and the HTL does not appear to have a detrimental effect on the carrier injection efficiency. As ob-

served earlier, the turnon voltages of both our SWNT-OLED and ITO-OLED devices are similar although greater organic layer thicknesses generally result in higher turnon voltages. Thus, as a first approximation, our results suggest that hole injection barriers for both ITO and SWNT anodes are similar. This was expected given the similar work function of SWNTs and ITO. However, it is clear that in addition to hole injection barriers, the adhesion and wetting characteristics of the deposited organic layers is central to the performance of SWNT-OLEDs.

In summary, we have implemented carbon nanotube anodes in small molecule OLED devices. Using this electrode material it is readily possible to achieve performances comparable to established ITO-based OLEDs. Unlike ITO, which is brittle, subject to cracking and delamination, carbon nanotube anodes are entirely flexible. Secondly, their room temperature processing renders them suitable for use with a wide range of substrates for both top and bottom emission devices. Finally, the nanoscale morphology of our electrode may yield alternative light outcoupling pathways. By optimizing the SWNT-HTL interface and increasing the carbon nanotube anode transparency, we believe that devices exhibiting performances superior to traditional ITO-based devices will soon be demonstrated.

The authors thank Dr. Benoit Simard and his group from the NRC for providing the SWNTs. They also gratefully acknowledge the financial support of the NSERC, the Canada Research Chair program, and the FQRNT during the course of this research.

- ¹L. S. Hung and C. H. Chen, *Mater. Sci. Eng.*, **R**, **39**, 143 (2002).
- ²G. G. Malliaras and J. C. Scott, *J. Appl. Phys.*, **83**, 5399 (1998).
- ³H. Aziz and Z. D. Popovic, *Chem. Mater.*, **16**, 4522 (2004).
- ⁴J. Cui, A. Wang, N. L. Edleman, J. Ni, P. Lee, N. R. Armstrong, and T. J. Marks, *Adv. Mater. Res. (N.Y.)*, **13**, 1476 (2001).
- ⁵P. Melpignano, A. Baron-Toaldo, V. Biondo, S. Priante, R. Zamboni, M. Murgia, S. Caria, L. Gregoratti, A. Barinov, and M. Kiskinova, *Appl. Phys. Lett.*, **86**, 041105 (2005).
- ⁶D. R. Cairns, R. P. Witte II, D. K. Sparacin, S. M. Sachsman, D. C. Paine, G. P. Crawford, and R. R. Newton, *Appl. Phys. Lett.*, **76**, 1425 (2000).
- ⁷S. Han, X. Feng, Z. H. Lu, D. Johnson, and R. Wood, *Appl. Phys. Lett.*, **82**, 2715 (2003).
- ⁸Z. C. Wu, Z. H. Chen, X. Du, J. M. Logan, J. Sippel, M. Nikolou, K. Kamaras, J. R. Reynolds, D. B. Tanner, A. F. Hebard, and A. G. Rinzler, *Science*, **305**, 1273 (2004).
- ⁹B. Shan and K. Cho, *Phys. Rev. Lett.*, **94**, 236602 (2005).
- ¹⁰V. Barone, J. E. Peralta, J. Uddin, and G. E. Scuseria, *J. Chem. Phys.*, **124**, 024709 (2006).
- ¹¹C. C. Wu, C. I. Wu, J. C. Sturm, and A. Kahn, *Appl. Phys. Lett.*, **70**, 1348 (1997).
- ¹²T. Takenobu, T. Takano, M. Shiraishi, Y. Murakami, M. Ata, H. Kataura, Y. Achiba, and Y. Iwasa, *Nat. Mater.*, **2**, 683 (2003).
- ¹³M. Zhang, S. Fang, A. A. Zakhidov, S. B. Lee, A. E. Aliev, C. D. Williams, K. R. Atkinson, and R. H. Baughman, *Science*, **309**, 1215 (2005).
- ¹⁴A. D. Pasquier, H. E. Unalan, A. Kanwal, S. Miller, and M. Chhowalla, *Appl. Phys. Lett.*, **87**, 203511 (2005).
- ¹⁵C. T. Kingston, Z. J. Jakubek, S. Denomme, and B. Simard, *Carbon*, **42**, 1657 (2004).
- ¹⁶J. Liu, A. G. Rinzler, H. J. Dai, J. H. Hafner, R. K. Bradley, P. J. Boul, A. Lu, T. Iverson, K. Shelimov, C. B. Huffman, F. Rodriguez-Macias, Y. S. Shon, T. R. Lee, D. T. Colbert, and R. E. Smalley, *Science*, **280**, 1253 (1998).
- ¹⁷J. G. C. Veinot and T. J. Marks, *Acc. Chem. Res.*, **38**, 632 (2005).
- ¹⁸E. Artukovic, M. Kaempgen, D. S. Hecht, S. Roth, and G. Gruner, *Nano Lett.*, **5**, 757 (2005).

Applied Physics Letters is copyrighted by the American Institute of Physics (AIP). Redistribution of journal material is subject to the AIP online journal license and/or AIP copyright. For more information, see <http://ojps.aip.org/aplo/aplcr.jsp>